


 Cite this: *RSC Adv.*, 2018, **8**, 12785

# A ratiometric fluorescence assay for acetylcholinesterase activity and inhibitor screening based on supramolecular assembly induced monomer–excimer emission transition of a perylene probe<sup>†</sup>

Chunhua He,<sup>ab</sup> Huipeng Zhou,<sup>\*b</sup> Ejaz Hussain,<sup>bc</sup> Yunyi Zhang,<sup>bd</sup> Niu Niu,<sup>bc</sup> Yunhui Li,<sup>a</sup> Yugui Ma<sup>ID \*a</sup> and Cong Yu<sup>\*bc</sup>

A ratiometric fluorescence assay for acetylcholinesterase activity is established, which is based on controlled perylene probe assembly and monomer–excimer transition. In a buffer solution, a perylene probe with two negatively charged groups (PDI-DHA) mainly exists in monomeric form. In the presence of cationic lauroylcholine and lauric acid, PDI-DHA can form supramolecular assemblies and the perylene excimer emission can be observed. AChE can catalyze the hydrolysis of lauroylcholine to anionic lauric acid and choline. The hydrolysis process can trigger the breakdown of the supramolecular assemblies. The perylene excimer recovers to the monomeric form because of the de-aggregation of the probe. The excimer–monomer transition can be detected, and a ratiometric fluorescence assay for AChE activity and inhibitor screening is therefore established.

Received 9th February 2018  
 Accepted 19th March 2018

DOI: 10.1039/c8ra01274a  
[rsc.li/rsc-advances](http://rsc.li/rsc-advances)

## Introduction

Acetylcholinesterase (AChE) is an important member of the carboxylesterase family that plays an essential role in the catalysis of hydrolysis of the neurotransmitter acetylcholine (ACh) localized in the central and peripheral nervous systems of animals.<sup>1</sup> Thus it maintains the level of ACh. The process is a pivotal step to control the neural response.<sup>2–4</sup> The function of brain neurons can be damaged as a result of dysfunction of acetylcholine. Its deficiency or elevation can induce vital diseases such as decreased heart rate, dilation of the blood vessel, and Alzheimer's disease (AD).<sup>5</sup> The decrease in the level of ACh from the standard levels in the cortex and hippocampus,<sup>6</sup> could help the assembly of amyloid  $\beta$  peptides into amyloid fibrils, which results in Alzheimer's disease (AD).<sup>7–11</sup> In fact, AChE plays an essential role in the development of AD. AChE inhibitors are usually used for the inhibition of ACh hydrolysis and increase the ACh concentration. The AChE

inhibitors are currently used as a principal drug for Alzheimer's disease and neuromuscular disorders.<sup>12–15</sup> Therefore, development of highly sensitive methods for the detection of AChE activity and screening of its potential inhibitor has great practical significance.

In the past decades, various assays for AChE activity and screening for potential inhibitors of AChE have been established. For example, the electrochemical,<sup>16,17</sup> colorimetric,<sup>18</sup> chemiluminescent,<sup>19</sup> and fluorometric assays, *etc.*<sup>20,21</sup> Various fluorescent materials have been tested to improve the detection of AChE activity and screening of its inhibitors. Such as CdS quantum dots,<sup>22</sup> gold nanoparticles,<sup>23</sup> and aromatic dyes.<sup>24</sup> Among them, organic fluorophores are highly attractive because of their high thermal and photochemical stability, longer lifetime and higher quantum yield.<sup>25,26</sup>

Perylene diimide (PDI) derivatives are one of the outstanding large planar  $\pi$ -conjugated molecules possessing excellent optical and electronic properties.<sup>24,27,28</sup> Furthermore, PDI derivatives as promising fluorescent probes have been applied to the biological analysis and sensing applications.<sup>29–31</sup> PDI derivatives have higher aggregation tendency due to strong  $\pi$ – $\pi$ , or  $\pi$ –C–H interactions and hydrophobic interactions. It results in the fluorescence quenching of monomers or turn-on excimer emission.<sup>32</sup> Over last few years, our group has reported studies on the PDI derivatives based fluorescent sensors.<sup>33–37</sup> In particular, PDI derivatives could be introduced into aggregation by polycation or polyanion, which result in excimer emission.<sup>38,39</sup> However, small molecules like

<sup>a</sup>Changchun University of Science and Technology, Weixing Road, No. 7989, Changchun 130022, P. R. China. E-mail: myq9393@sina.com

<sup>b</sup>State Key Laboratory of Electroanalytical Chemistry, Changchun Institute of Applied Chemistry, Chinese Academy of Sciences, Changchun, 130022, P. R. China. E-mail: congyu@ciac.ac.cn; hzhou@ciac.ac.cn

<sup>c</sup>University of the Chinese Academy of Sciences, Beijing, 100049, P. R. China

<sup>d</sup>School of Materials Science and Engineering, Tianjin University, Tianjin, 300072, PR China

<sup>†</sup> Electronic supplementary information (ESI) available. See DOI: 10.1039/c8ra01274a



lauroylcholine have not been reported to induce the excimer emission of PDI derivatives.

Herein, we report a novel strategy to induce PDI excimer by a small molecule rather than a polymer for the first time. And we have successfully developed a sensitive ratiometric fluorescence assay for AChE activity based on the controlled PDI assembly and monomer-excimer transition. The illustrative diagram of our detection strategy is depicted in Scheme 1 (1) In a buffer solution, a water-soluble probe (PDI-DHA) mainly exists in monomeric form due to the negative charge electrostatic repulsive interactions. The monomer emission peak of PDI-DHA appears at 548 nm. (2) Lauroylcholine is employed as the substrate of AChE. The probe molecules aggregate to form supramolecular assemblies, when mixed with lauroylcholine and lauric acid. As a result, a redshifted emission appears at a wavelength of 680 nm which belongs to the excimer of PDI-DHA. (3) AChE can catalyze the hydrolysis of lauroylcholine to lauric acid and choline. The hydrolysis process can trigger the breakdown of the supramolecular assemblies because of the electrostatic repulsion between lauric acid and PDI-DHA. The PDI-DHA excimer transfers to the monomeric form because of the de-aggregation of the probe. The excimer-monomer transition can be detected, and a ratiometric fluorescence method for AChE activity is accomplished. When an AChE inhibitor is present, AChE activity is significantly retarded, and a lesser level of excimer-monomer transition is observed. Thus our method can be used for screening the inhibitors of AChE.

## Experimental section

### Materials and measurements

PDI derivative (PDI-DHA) was prepared and purified according to the previous procedures.<sup>40</sup> Lauroylcholine was bought from Aladdin (Shanghai, China). Lauric acid was purchased from Dayang Chemicals Co., Ltd. Trypsin and acetylcholinesterase was ordered from Sigma. S1 nuclease and Lysozyme was bought from Fermentas Inc. (MBI, Canada). Alkaline phosphatase (ALP), BSA, exonuclease I (Exo I) were obtained from Takara Biotechnology Co., Ltd. 3-Hydroxycarbofuran, and donepezil hydrochloride were bought from J & K Scientific Ltd. Deionized water purified by a Milli-Q A10 system (Millipore, Billerica, MA, USA) was used for sample preparation. Fluoromax-4 spectrophotofluorometer (Horiba Jobin Yvon Inc., USA) was employed to

record fluorescence emission and excitation spectra with 5 nm slit. The emission spectra of PDI-DHA were obtained at an excitation wavelength of 488 nm in a quartz cuvette with 10 mm path length and 2 mm window width. The particle size distribution was investigated by dynamic light scattering method by using zetasizer nano ZS-90, particle size and zeta potential analyzer (Malvern Instruments, UK).

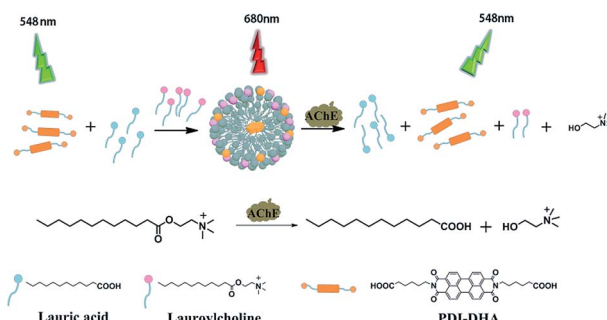
### Assay procedures

2.6  $\mu$ L of lauroylcholine (20 mM) was added to MOPS buffer (pH 7.5, 10 mM), and AChE in a fixed concentration was added (sample volume, 373.4  $\mu$ L). The sample mixture was incubated at 37 °C for 180 min. Then, 6.6  $\mu$ L of lauric acid (20 mM) and 20  $\mu$ L of PDI-DHA (200  $\mu$ M) was added. The final sample volume was 400  $\mu$ L and the emission spectra were recorded at 20 °C.

## Results and discussion

### Design and optimization of the assay

PDI derivative (PDI-DHA) with two negative charges was synthesized according to the previous procedure.<sup>40</sup> In the buffer solution, PDI-DHA displays unique monomer emission with peaks at 548 and 587 nm. The amphiphilic compound lauroylcholine was employed to be a good substrate for AChE and introduce the PDI-DHA aggregation. So that it showed a broad excimer emission band at around 680 nm. The critical micelle concentration (CMC) of lauroylcholine was determined by using pyrene as a probe and illustrated in Fig. S1 (ESI†). The  $I_{392}/I_{370}$  ratio of the pyrene fluorescence emission spectra as a function of lauroylcholine concentration gave the CMC value of 0.612 mM at 20 °C. According to the literature, surfactants can form supramolecular assemblies in aqueous solutions, and the critical aggregation concentration (CAC) of a surfactant could be reduced in the presence of counterions.<sup>41,42</sup> In this paper, PDI-DHA was used as a counterion to reduce the CAC of lauroylcholine due to its strong electrostatic interactions. In addition, 10  $\mu$ M of PDI-DHA was preferentially prepared in the MOPS buffer solution (10 mM, pH 7.5), which is significant for excimer formation. As illustrated in Fig. 1, PDI-DHA showed typical monomer emission with peaks at 548 and 587 nm in the absence or lower concentration of lauroylcholine. A new and broad emission band with a peak at 680 nm could be observed, and the intensity gradually enhanced with the gradual increase



Scheme 1 Schematic illustration of the ratiometric fluorometric assay for acetylcholinesterase activity detection.

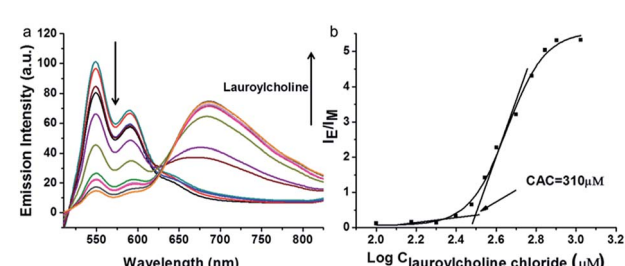


Fig. 1 (a) Changes in emission spectra of PDI-DHA (10  $\mu$ M) in the presence of different concentrations (0–800  $\mu$ M) of lauroylcholine. (b) Corresponding  $I_E/I_M$  value changes of PDI-DHA (10  $\mu$ M) as a function of lauroylcholine concentration.



of lauroylcholine concentration (0–800  $\mu\text{M}$ ). PDI-DHA and lauroylcholine could form supramolecular assemblies due to electrostatic interactions, resulting in a CAC value of 310  $\mu\text{M}$  for lauroylcholine. However, in this case, the concentration of enzyme substrate (lauroylcholine) remains high for the AChE activity detection and the sensitivity may be limited.

Herein, we selected lauric acid as the alternate counterion to reduce the concentration of lauroylcholine. As shown in Fig. 2, 130  $\mu\text{M}$  of lauroylcholine which was lower than its CAC, 10  $\mu\text{M}$  of PDI-DHA and varying amounts of lauric acid (100–500  $\mu\text{M}$ ) were added.

With the increase of the amount of lauric acid, the monomer emission decreased and excimer emission increased gradually. When 300  $\mu\text{M}$  lauric acid was added, the value of intensity ratio ( $I_E/I_M$ , in which  $I_E$  and  $I_M$  refer to the emission intensities at 680 nm and 548 nm, respectively) reached its maximum. Fig. 2b illustrates the stable assemblies of 10  $\mu\text{M}$  PDI-DHA and 300  $\mu\text{M}$  lauric acid in the presence of 130  $\mu\text{M}$  (much lower than 310  $\mu\text{M}$ ) of lauroylcholine.

For optimal AChE activity detection, the concentration of lauroylcholine should be as low as possible. The concentration of PDI-DHA was fixed at 10  $\mu\text{M}$ . The fluorescence spectra of supramolecular assemblies were interrogated with the fixed ratio of [lauroylcholine]: [lauric acid] = 130  $\mu\text{M}$ : 300  $\mu\text{M}$ . As shown in Fig. S2,<sup>†</sup> the intensity ratio (the  $I_E/I_M$  value) increased gradually with the increase of lauroylcholine concentration. When the concentration of lauroylcholine was 130  $\mu\text{M}$ , the  $I_E/I_M$  value reached its maximum. A further increase of the concentration of the mixture of lauroylcholine/lauric acid (130  $\mu\text{M}$ /300  $\mu\text{M}$ ) caused no increase of the  $I_E/I_M$  value, indicating that most of the PDI-DHA molecules had been transformed to the aggregated form.

Meanwhile, both PDI-DHA and lauric acid contained carboxylic acid groups. Thus the supramolecular aggregation in mixed solutions can be controlled by varying the pH of the system. We investigated the fluorescence intensity ratio (the  $I_E/I_M$  value) in different pH buffer (see Fig. S3<sup>†</sup>). When the pH value is greater than 8.0, the PDI-DHA molecules may not aggregate. And when the pH value is 7.5, the  $I_E/I_M$  value of PDI-DHA reached the maximum in the assay system containing lauric acid (300  $\mu\text{M}$ ) and lauroylcholine (130  $\mu\text{M}$ ). The optimal pH value was chosen to be 7.5 throughout the whole experiment.

We also investigated the optimal concentration of PDI-DHA with the assay system containing lauroylcholine (130  $\mu\text{M}$ ) and

lauric acid (300  $\mu\text{M}$ ). As shown in Fig. S4,<sup>†</sup> different concentrations (5, 10, 20, 30  $\mu\text{M}$ ) of PDI-DHA were added, it was difficult to get the excimer emission when the concentrations were too low. When the concentration of PDI-DHA was 10  $\mu\text{M}$ , the  $I_E/I_M$  value reached its maximum. Therefore the optimal concentration of PDI-DHA was chosen to be 10  $\mu\text{M}$ .

## Characterization of supramolecular assembly

The average size distribution of the supermolecular assembly was characterized in MOPS buffer by Dynamic Light Scattering at 25 °C. As shown in Fig. S5,<sup>†</sup> the results confirmed that the supramolecular assemblies could not be formed in the absence of the PDI-DHA, lauric acid or lauroylcholine chloride. The supramolecular assemblies with sizes around 414 nm could be measured in the mixed solution when the three components present simultaneously.

## Supramolecular assemblies triggering the development of AChE activity assay

AChE can hydrolyze lauroylcholine into lauric acid and choline, the amount of lauroylcholine will decrease with the addition of AChE. The hydrolysis process can trigger the breakdown of the supramolecular complex as a result of the coulombic repulsive interactions between negatively charged PDI-DHA and lauric acid. The monomeric emission of PDI-DHA is a turn-on because of the excimer–monomer transition due to de-aggregation. Thus, the ratio of excimer and monomer could be used to monitor the process of enzymatic hydrolysis. The time-dependence of the resulting sample was tested by recording the fluorescence spectra at regular time intervals (Fig. 3). In the presence of 150 mU mL<sup>−1</sup> AChE, with the prolongation of time, the lauroylcholine was consumed, and the ratio of lauroylcholine and lauric acid continuously changed. Resulting in the transition of the PDI-DHA monomer state and excimer state. The excimer emission decreased gradually, meanwhile, the monomer emission increased gradually with increasing enzymatic reaction time. It is worth noting that there is no clear isoemissive point at around 640 nm because it is a more complex system than the simple two-component excimer–monomer equilibrium.<sup>43</sup> Maximum  $I_M/I_E$  value was observed after 180 min of enzymatic reaction (Fig. 3b). Therefore, 180 min was selected as the optimal enzyme reaction time.

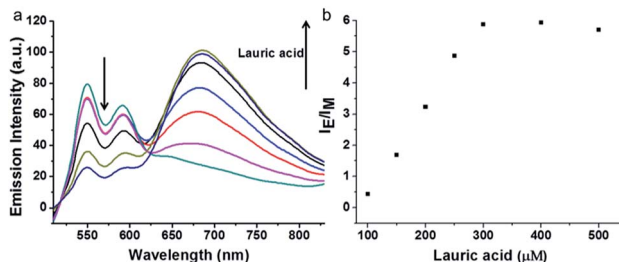


Fig. 2 Changes in emission spectra (a) and corresponding  $I_E/I_M$  value (b) of PDI-DHA (10  $\mu\text{M}$ ) and lauroylcholine (130  $\mu\text{M}$ ) in the presence of the different concentrations (100–500  $\mu\text{M}$ ) of lauric acid.

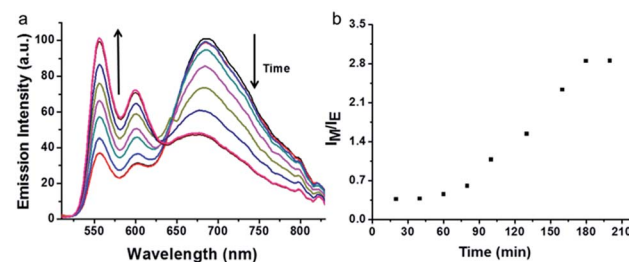


Fig. 3 Emission spectra (a) and the corresponding  $I_M/I_E$  value (b) changes as a function of the enzymatic reaction time. Conditions: AChE = 120 mU mL<sup>−1</sup>, lauric acid = 300  $\mu\text{M}$ , lauroylcholine = 130  $\mu\text{M}$ .



Our assay could be used to qualify the concentration of AChE. The changes in fluorescence emission of the supramolecular assemblies were monitored by varying the concentration of AChE. Fixed concentration of lauroylcholine (130  $\mu\text{M}$ ) and different concentrations of AChE (0, 5, 10, 20, 40, 60, 80, 100, 150, 200, 250  $\text{mU mL}^{-1}$ ) were mixed. The mixture was placed in 37 °C water bath for 180 min, after hydrolysis reaction, lauric acid (300  $\mu\text{M}$ ) and PDI-DHA (10  $\mu\text{M}$ ) were added. The fluorescence emission was detected at 20 °C. As shown in Fig. 4, with an increase in the concentration of AChE, the monomer emission intensity of PDI-DHA increased gradually. The emission intensity ratios ( $I_{\text{M}}/I_{\text{E}}$ ) of PDI-DHA plotted against the concentrations of AChE, which displayed a linear relationship at AChE concentration range of 5–150  $\text{mU mL}^{-1}$ . The linear correlation equation is  $\text{IF} = 0.0914 + 0.0204 [\text{AChE}]$ ,  $R^2 = 0.999$ . Where “IF” refers to the emission intensity ratio of the  $I_{\text{M}}/I_{\text{E}}$ , and “[AChE]” refers to the concentration of AChE. Our method had a better sensitivity and 5  $\text{mU mL}^{-1}$  AChE could be easily detected.<sup>44–48</sup>

### Selectivity of the assay

To examine the specificity of the AChE activity assay, the fluorescence response of lauroylcholine towards various enzymes and proteins, including ALP, S1 nuclease, lysozyme, Exo I nuclease, trypsin, and BSA were recorded. The concentrations of ALP, S1 nuclease, lysozyme, Exo I nuclease and trypsin were kept at 1  $\text{U mL}^{-1}$ , and the concentrations of BSA was 1  $\text{mg mL}^{-1}$ . The samples were incubated for 180 min under the same conditions as for AChE. From Fig. 5, compared the value of  $I_{\text{M}}/I_{\text{E}}$  for AChE (150  $\text{mU mL}^{-1}$ ) with that of other substances (1  $\text{U mL}^{-1}$ ). Significant changes were only seen for AChE. Other enzymes and proteins gave no noticeable monomer intensity recovery. The results suggest that our assay is highly selective for AChE, and could be applied to detect AChE activity in the presence of other enzymes.

### Inhibitor screening of the assay

It is a fact that the activity of AChE to hydrolyze lauroylcholine could be restrained when an AChE inhibitor existed. The inhibitors of AChE were widely applied as drugs for the treatment of Alzheimer's disease (AD) *via* increasing the amounts of acetylcholine. Therefore, screening for AChE potential inhibitor is of great value. In order to confirm the potential application of

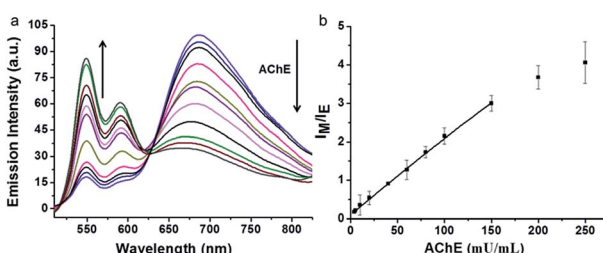


Fig. 4 (a) Fluorescence spectra changes of the assembly in the presence of different concentrations of AChE (5–250  $\text{mU mL}^{-1}$ ). (b) Corresponding  $I_{\text{M}}/I_{\text{E}}$  value based calibration curve for AChE (5–250  $\text{mU mL}^{-1}$ ).

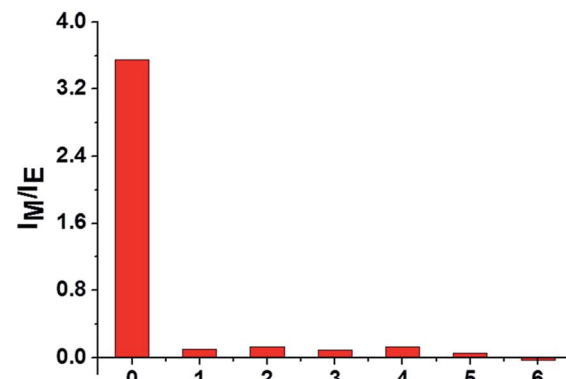


Fig. 5 Selectivity study.  $I_{\text{M}}/I_{\text{E}}$  values of the PDI-DHA in the presence of AChE and the other proteins. Columns 0–6: AChE, ALP, S1 nuclease, lysozyme, Exo I nuclease, trypsin, and BSA. AChE: 150  $\text{mU mL}^{-1}$ ; other enzymes: 1  $\text{U mL}^{-1}$ , BSA: 1  $\text{mg mL}^{-1}$ . Background is deducted.

the assay for AChE inhibitor screening, 3-hydroxycarbofuran and donepezil, two typical inhibitors of AChE were tested.<sup>46</sup> The fluorescence emission spectra of PDI-DHA with different concentration of both inhibitors were investigated (Fig. S6a and S7a†). The Fig. S6b and S7b† showed that the  $I_{\text{M}}/I_{\text{E}}$  value reduced with the enhancement of the amounts of 3-hydroxycarbofuran and donepezil. The results indicate that the 3-hydroxycarbofuran and donepezil were more effective at higher concentrations. And the  $\text{IC}_{50}$  values of 3-hydroxycarbofuran and donepezil were estimated to be 149.2 nM and 57.5 nM, respectively. The results clearly suggest that our assay can be applied for inhibitor screening.

To further investigate the applicability of the supramolecular assemblies for screening AChE inhibitors. Lake water samples were used. Different concentrations of the AChE inhibitors 3-hydroxycarbofuran (50, 100, 200, 300, 400, 500 nM) and donepezil (25, 50, 100, 150, 200 nM) were added to the lake water samples. Their inhibition effects were compared with those in the buffer solution. As shown in Fig. 6, the inhibition effect of the samples prepared in the lake water is similar to those prepared in buffer solution. The results suggest that our assay can be applied for the screening of AChE inhibitors in real samples.

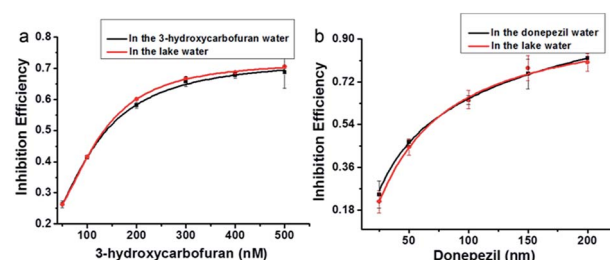


Fig. 6 Plot of the inhibition efficiency as a function of 3-hydroxycarbofuran (50, 100, 200, 300, 400, 500 nM) (a) and donepezil (25, 50, 100, 150, 200 nM) (b) concentration. Samples were prepared in deionized water (black line) or lake water (red line).

## Conclusions

In summary, we report a ratiometric fluorescence method for the detection of AChE activity and its inhibitor screening based on the formation of a supramolecular assembly of a PDI derivative in the presence of small molecules (lauric acid and lauroylcholine) for the first time. It is based on the monomer-excimer emission transition and the controlled release of PDI-DHA from the supramolecular assemblies. AChE can catalyze the hydrolysis of lauroylcholine to lauric acid and choline. The hydrolysis process can trigger the breakdown of the supramolecular assemblies. The perylene excimer changes to the monomeric. The excimer-monomer transition can be detected, and a ratiometric fluorescence method for AChE activity is established. The assay is facile, efficient and inexpensive, which also exhibits high sensitivity and selectivity. Our assay can also be applied for the screening of AChE inhibitors in real samples.

## Conflicts of interest

There are no conflicts to declare.

## Acknowledgements

This work was supported by the National Natural Science Foundation of China (21561162004), and the Science and Technology Development Project of the Jilin Province (20170204038GX).

## Notes and references

- 1 M. Palkovit and D. M. Jacobowi, *J. Comp. Neurol.*, 1974, **157**, 29–41.
- 2 H. Zejli, I. Naranjo-Rodriguez, B. Liu, K. R. Temsamani and J. L. Marty, *Talanta*, 2008, **77**, 217–221.
- 3 J. W. Mason, C. L. Schmid, L. M. Bohn and W. R. Roush, *J. Am. Chem. Soc.*, 2017, **139**, 5865–5869.
- 4 G. S. M. Hanan, Y. W. Barbas, E. K. Hussain and Y. Shoham, *Brain Struct. Funct.*, 2013, **218**, 59–72.
- 5 A. V. Terryjr and J. J. Buccafusco, *J. Pharmacol. Exp. Ther.*, 2003, **306**, 821–827.
- 6 A. M. S. Kar, D. Issa, D. S. Seto, B. Auld, R. Collier and J. Quirion, *Neurochem*, 1998, **70**, 2179–2187.
- 7 M. Singh, M. Kaur, H. Kukreja, R. Chugh, O. Silakari and D. Singh, *Eur. J. Med. Chem.*, 2013, **70**, 165–188.
- 8 L. A. Arribas, M. A. Lomillon, O. D. Renedo and M. J. Martínez, *Talanta*, 2013, **111**, 8–12.
- 9 M. H. Pournaghi-Azar and A. Saadatirad, *J. Electroanal. Chem.*, 2008, **624**, 293–298.
- 10 R. L. Zhang, S. S. Liang, M. Jin, T. He and Z. Q. Zhang, *Sens. Actuators, B*, 2017, **253**, 196–202.
- 11 A. Makower, C. R. Lowe and F. W. Scheller, *J. Anal. Chem.*, 1999, **364**, 179–183.
- 12 M. B. Colovic, D. Z. Krstic, T. D. Lazarevic-Pasti, A. M. Bondzic and V. M. Vasic, *Curr. Neuropharmacol.*, 2013, **1**, 3–6.
- 13 J. W. Mason, C. L. Schmid, L. M. Bohn and W. R. Roush, *J. Am. Chem. Soc.*, 2017, **139**, 5865–5869.
- 14 E. Kozma and M. Catellani, *Dyes Pigm.*, 2013, **98**, 160–179.
- 15 L. P. Köse and I. Gulcin, *Rec. Nat. Prod.*, 2017, **11**, 558–561.
- 16 H. Wang, J. Wang, C. Timchalk and Y. H. Lin, *Anal. Chem.*, 2008, **80**, 8477–8484.
- 17 D. Du, Y. Tao, W. Y. Zhang, D. L. Liu and H. B. Li, *Biosens. Bioelectron.*, 2011, **26**, 4231–4235.
- 18 M. Wang, X. G. Gu, G. X. Zhang, D. Q. Zhang and D. B. Zhu, *Langmuir*, 2009, **25**, 2504–2507.
- 19 S. Sabelle, P. Y. Renard, K. Pecorella, S. S. Dezard, C. Creminon, J. Grassi and C. Mioskowski, *J. Am. Chem. Soc.*, 2002, **124**, 4874–4880.
- 20 E. Golub, R. Freeman and I. Willner, *Anal. Chem.*, 2013, **85**, 12126–12133.
- 21 K. Ma, L. Lu, Z. Qi, J. Feng, C. Zhuo and Y. Zhang, *Biosens. Bioelectron.*, 2015, **68**, 648–653.
- 22 R. Gill, L. Bahshi, B. Freeman and I. Willner, *Angew. Chem., Int. Ed.*, 2008, **47**, 1676–1679.
- 23 V. Pavlov, Y. Xiao and I. Willner, *Nano Lett.*, 2005, **5**, 649–653.
- 24 E. Hussain, H. Zhou, N. Yang, S. A. Shahzad and C. Yu, *Dyes Pigm.*, 2017, **147**, 211–224.
- 25 L. Z. Gai, H. C. Chen, B. Zou, H. Lu, G. Q. Lai, Z. F. Li and Z. Shen, *Chem. Commun.*, 2012, **48**, 10721–10723.
- 26 Y. D. Zhang, Y. N. Cai, Z. L. Qi, L. Lu and Y. X. Qian, *Anal. Chem.*, 2013, **85**, 8455–8461.
- 27 M. Wang, X. G. Gu, G. X. Zhang, D. Q. Zhang and D. B. Zhu, *Anal. Chem.*, 2009, **81**, 4444–4449.
- 28 P. R. L. Malenfant, C. D. Dimitrakopoulos, J. D. Gelorme, L. L. Kosbar, T. O. Graham, A. Curioni and W. Andreoni, *Appl. Phys. Lett.*, 2002, **80**, 2517–2519.
- 29 G. Grisci, E. Kozma, K. Pagano, L. Ragona and F. Galeotti, *RSC Adv.*, 2016, **6**, 64374–64382.
- 30 Z. J. Chen, L. M. Wang, G. Zou, L. Zhang, G. J. Zhang, X. F. Cai and M. S. Teng, *Dyes Pigm.*, 2012, **94**, 410–415.
- 31 S. S. Zhang, X. J. Wang, Y. W. Huang, H. Y. Zhai and Z. H. Liu, *Sens. Actuators, B*, 2018, **254**, 805–810.
- 32 Q. F. Yan, Y. Zhou, Y. Q. Zheng, J. Pei and D. H. Zhao, *Chem. Sci.*, 2013, **4**, 4389–4395.
- 33 D. L. Liao, J. Chen, H. P. Zhou, Y. Wang, Y. X. Li and C. Yu, *Anal. Chem.*, 2013, **85**, 2667–2672.
- 34 J. Chen, D. L. Liao, Y. Wang, H. P. Zhou, W. Y. Li and C. Yu, *Org. Lett.*, 2013, **15**, 2133–2135.
- 35 Y. Y. Zhang, C. Y. Zhang, J. Chen, Y. X. Li, M. D. Yang, H. P. Zhou, S. A. Shahzad, H. Qi, C. Yu and S. H. Jiang, *J. Mater. Chem. C*, 2017, **5**, 4691–4694.
- 36 Y. Chen, W. Y. Li, Y. Wang, X. D. Yang, J. Chen, Y. G. Jiang, C. Yu and Q. Lin, *J. Mater. Chem. C*, 2014, **2**, 4080–4085.
- 37 Y. Wang, J. Chen, Y. Chen, W. Y. Li and C. Yu, *Anal. Chem.*, 2014, **86**, 4371–4378.
- 38 Y. J. Wu, P. H. Ni, M. Z. Zhang and X. L. Zhu, *Soft Matter*, 2010, **6**, 3751–3758.
- 39 M. Wathier, B. A. Lakin, P. N. Bansal, S. S. Stoddart, B. D. Snyder and M. W. Grinstaf, *J. Am. Chem. Soc.*, 2013, **135**, 4930–4933.
- 40 Y. Wang, J. Chen, H. Jiao, Y. Chen, W. Li, Q. Zhang and C. Yu, *Chem.-Eur. J.*, 2013, **19**, 12846–12852.



41 E. N. Savariar, S. Ghosh, D. C. Gonzalez and S. Thayumanavan, *J. Am. Chem. Soc.*, 2008, **130**, 5416–5417.

42 D. C. Gonzalez, E. N. Savariar and S. Thayumanavan, *J. Am. Chem. Soc.*, 2009, **131**, 7708–7716.

43 S. Nagatoishi, T. Nojima, B. Juskowiak and S. Takenaka, *Angew. Chem., Int. Ed.*, 2005, **117**, 5195–5198.

44 F. D. Feng, Y. L. Tang, S. Wang, Y. L. Li and D. B. Zhu, *Angew. Chem., Int. Ed.*, 2007, **46**, 7882–7886.

45 X. Shen, F. X. Liang, G. X. Zhang and D. Q. Zhang, *Analyst*, 2012, **137**, 2119–2123.

46 D. J. Selkoe, *Physiol. Rev.*, 2001, **81**, 741–766.

47 C. Ye, M. Q. Wang, X. Zhong, S. H. Chen, Y. Y. Chai and R. Yuan, *Biosens. Bioelectron.*, 2016, **79**, 34–40.

48 K. Ingkaninan, P. Temkitthawon, K. Chuenchom, T. Yuyaem and W. Thongnoi, *J. Ethnopharmacol.*, 2003, **89**, 261–264.

